Effects of Temperature on Membrane Electrodiffusion

Oscar Patterson[1], Ramón Martínez[2], Ilyssa Summer[3]
Jose Barrios[1], Mayteé Cruz-Aponte[3], Marco Arieli Herrera-Valdez[3]

[1] Montclair State University, NJ, USA,

[2] Universidad de Sonora, Sonora, México,

[3] Arizona State University, AZ, USA

August 17, 2010

Abstract

From a theoretical point of view, many cell functions such as action potential generation and general signaling depend on molecular transport across their membrane. In this work we aim to increase our understanding of how the properties of membrane transport depend on temperature. To start addressing this problem, we use a thermodynamical description of ionic flow across membranes. With this we model two processes of high relevance: cellular excitability and regulation of extracellular pH. We use dynamical systems theory to analyze the behavior of the system with respect to temperature. We specifically address the following questions: (1) does temperature affect the dynamics of action potential generation and firing frequency? (2) what is the dependence of the transmembrane acidity levels on body temperature? In regard to excitability, we expect to describe the behavior of neurons and other excitable cells in cold blooded animals as the environment temperature changes. In addition, one potentially interesting aspect of our findings in regard to pH regulation is to unravel mechanisms explaining why temperature-based therapies work for the treatment of some cancers.

1 Introduction

In this work we study how some physical parameters, specially temperature, affects membrane transport. In order to study this we have taken a biophysical approach. We have used an equation derived from thermodynamical and electrodiffusion considerations to describe flux across the membrane. With these equations we have studied the role of temperature in two interesting cases. First, we address the flow of potassium and sodium ions in the neuronal membrane that is involved in the generation of action potentials. Then we decided to study the regulation of pH in the extracellular medium which is believed to be related to cancer [5].

2 Biophysical background

In this section we make an outline of the ideas first developed by Goldman and then by Endresen in [8] to build equations for flow of ions through the membrane.

2.1 Nernst potential

Nearly impermeable to the passage of ions, the cell membrane consists of differing concentrations of ions inside and outside the cell (i.e., an ion concentration gradient). Similar to the charged perfect conductor of electrostatics, the intracellular ions tend to concentrate near the membrane. These attract oppositely charged extracellular ions to produce an electric potential gradient in addition to the concentration gradient.

Embedded in the membrane are ion-specific channels mediating diffusion. As described by Fick's law, the diffusive flow across the membrane can be written as:

$$\vec{\phi}_{diff} = -ukT\nabla[\mathrm{S}], \tag{1}$$

where $\vec{\phi}$ is the ionic flux ($\frac{1}{M^2 s}$), [S] is the concentration of ions ($\frac{1}{m^3}$), u is the ion mobility ($\frac{\mathrm{mCN}}{\mathrm{s}}$), T is absolute temperature (K), and k is the Boltzmann's constant (J or Nm).

Simultaneously, Ohm's law governs the motion of charges in a potential gradient as:

$$\vec{\phi}_{ohm} = -zqu[\mathrm{S}]\nabla U, \tag{2}$$

where z is the valence of the ion species, q the elementary unit of charge, and U the electrical potential. Adding these two fluxes yields,

$$\vec{\phi}_{total} = -ukT\nabla[S] - uzq[S]\nabla U \tag{3}$$

$$= -ukT\exp\left(-\frac{zqU}{kT}\right)\nabla\left[[S]\exp\left(\frac{zqU}{kT}\right)\right]. \tag{4}$$

This is the Nernst-Planck equation for the total ion flux due to the electric force and diffusion. The derivation is given in appendix **A.1**.

To find the formula for the voltage at which the flux due to diffusion and the electrical force cancels, we set $\vec{\phi}_{total} = 0$ in the Nernst-Planck equation (3), separate U and $[S]$, and integrate from the extracellular to the intracellular side of the membrane

$$-uzq\int_{out}^{in}\frac{\partial U}{\partial x}dx = ukT\int_{out}^{in}\frac{1}{[S]}d[S]$$

$$\implies v_{\mathrm{S}} = U_{in} - U_{out} = \frac{kT}{zq}\ln\frac{[\mathrm{S}]_{out}}{[\mathrm{S}]_{in}}. \tag{5}$$

This is the Nernst potential for an ion species (also know as the reversal potential). It is the potential drop across the membrane, from the intracellular to the extracellular region, at which the net ion flux vanishes for a given $[\mathrm{S}]_{out}/[\mathrm{S}]_{in}$ and T.

2.2 Ion channel current

Consider an ion channel of length d and cross sectional area $A = A(x)$, where x is the distance from outside to inside and $A(x)$ varies with distance along the length of the channel. Importantly, the current I is assumed to be the same in cross section across the pore (i.e., independent of x) and is related to the x-component of the flux ϕ_x as follows:

$$I = qz\phi_x A, \qquad \text{or,} \quad \phi_x = \frac{I}{zqA}.$$

Equating the expresion above to the x-component of the Nernst-Planck equation (3) and multiplying by $\exp(zq(U - U_0)/kT$, where U_0 is the average of

the potentials at each end of the channel, yield

$$\frac{I}{A}\exp\left(\frac{zq(U-U_0)}{kT}\right) = -zqukT\frac{d}{dx}\left[[\mathrm{S}]\exp\left(\frac{zq(U-U_0)}{kT}\right)\right].$$

Integrating this last equation from the intracellular to the extracellular region (U, [S], and A are functions of x) and factoring out $\sqrt{[\mathrm{S}]_{out}[\mathrm{S}]_{in}}$ results in

$$I = \frac{2zqukT}{Q}\sqrt{[\mathrm{S}]_{out}[\mathrm{S}]_{in}}\sinh\left(\frac{ze(v-v_S)}{2kT}\right), \tag{6}$$

where

$$Q = \int_{in}^{out}\frac{1}{A}\exp\left(\frac{zq(U-U_0)}{kT}\right)dx. \tag{7}$$

The value of this integral is not known for the general case. However, we can address it for the next particular case: Suppose $U = U(x)$ is linear (i.e., the electric field is constant), and that the cross-sectional area $A(x)$ has a constant value A_0 except for a short, narrow pore in the center of area $A_p << A_0$ and length ϵd. We then obtain:

$$Q = \frac{2dkT}{zqv}\left[\frac{1}{A_0}\sinh\left(\frac{zqv}{2kT}\right) + \left(\frac{1}{A_p}-\frac{1}{A_0}\right)\sinh\left(\frac{\epsilon zqv}{2kT}\right)\right].$$

For ϵ and A_p sufficiently small, this may be approximated by a constant:

$$Q \approx Q_0 = \frac{\epsilon d}{A_p}.$$

Then, Eqn. (6) becomes

$$i = k_S\sinh\left(\frac{zq(v-v_S)}{2kT}\right) \tag{8}$$

where

$$k_S = 2zqukT\sqrt{[\mathrm{S}]_{out}[\mathrm{S}]_{in}}\frac{A_p}{\epsilon d}. \tag{9}$$

Here, k_S is independent of the membrane potential v. We use (8) as our model for ion channel currents.

2.3 Flux mediated by transporter proteins

The flux mediated by an exchanger protein taking m ions of type X from outside the cell in exchange for n ions of type Y from inside the cell can be thought of as the result of a reaction $mX_o + nY_i \rightleftharpoons mX_i + nY_o$ with forward rate α and backward rate β. The balance between the forward and backward rates can be expressed as

$$\frac{\alpha}{\beta} = \exp\left(\frac{\Delta G}{kT}\right) \tag{10}$$

where the change in free energy of the system is given by

$$\Delta G = q\left[mz_x(v - v_x) + nz_y(v - v_y)\right]. \tag{11}$$

As a consequence, the flux is described by writing $N(\alpha - \beta)$, which written in terms of the free energy of the system is

$$F = N\lambda(T)\sqrt{[X]_o^m[X]_i^m[Y]_o^n[Y]_i^n}\sinh\left[\frac{q}{2kT}(mz_x(v - v_x) + nz_y(v - v_y))\right]. \tag{12}$$

3 Applications

3.1 Application I: Neuron dynamics

We apply Eqn. (6) for the flux that we have derived in the last section to study the generation of action potential in the neuron membrane.

3.1.1 Mathematical model

Neurons can be thought as dynamical systems [7]. In neurons, the most important transmembrane fluxes are those of potassium K^+ and sodium Na^+. The extracellular medium has a high concentration of sodium ions, while the intracellular medium has a high concentration of potassium [7]. Figure 1 also depicts the channels through which ions flow. According to (8) the currents for sodium and potassium are of the form:

$$i_{Na} = A_{Na}\sinh\left(\frac{q}{2kT}(v - v_{Na})\right) \tag{13}$$

$$i_K = A_K\sinh\left(\frac{q}{2kT}(v - v_K)\right) \tag{14}$$

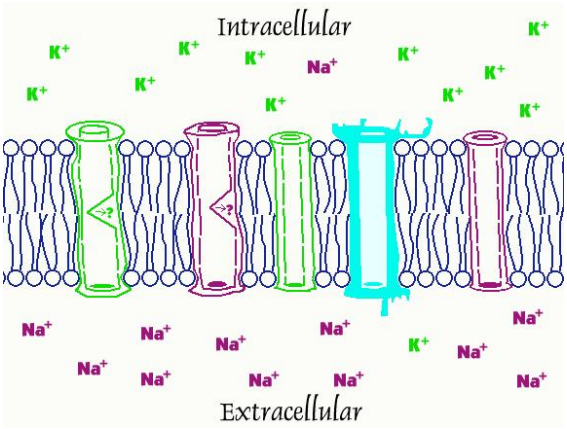

Figure 1: Inside the cell there is a higher concentration of potassium ions. In contrast the extracellular concentration of sodium is higher than it's intracellular counterpart. The figure also shows the channels through which ions diffuse (Figure taken from wikipedia commons).

The membrane can be modeled as a capacitor. As such, it has an associated capacitor current that will be equal and opposite to the sum of the channel currents, we obtain:

$$\begin{aligned} c_m \frac{dv}{dt} &= -i_{Na} - i_K \qquad (15) \\ &= -A_{Na} \sinh\left(\frac{q}{2kT}(v - v_{Na})\right) - A_K \sinh\left(\frac{q}{2kT}(v - v_k)\right). \end{aligned}$$

In addition, the potassium and sodium channels are voltage-gated. This is taken into account with the introduction of the gating variables $m(v), w(v) \in (0, 1)$ by writing:

$$A_{Na} = a_{Na} m^3 \qquad (16)$$
$$A_K = a_K w^4. \qquad (17)$$

After substitution of Eqns. (16)-(17) into Eqn. (16) and the factorization of the maximal current amplitude for Na^+, the equation for membrane potential becomes

$$\frac{dv}{dt} = \frac{\bar{a}_{Na}}{c_m}\left\{-m^3 \sinh\left[\frac{q(v - v_{Na})}{2kT}\right] - \frac{a_K}{a_{Na}} w^4 \sinh\left[\frac{q(v - v_K)}{2kT}\right]\right\} \qquad (18)$$

where the gate dynamics [7] are given by:

$$\frac{dm}{dt} = \frac{m_\infty(v) - m}{\tau_m(v)} \qquad (19)$$
$$\frac{dw}{dt} = \frac{w_\infty(v) - w}{\tau_w(v)}, \qquad (20)$$

with $\tau_m(v)$ and $\tau_w(v)$ representing the time constants for m and w, respectively. The steady states of m and w are, respectively, m_∞ and w_∞.
Fitz-Hugh was the first to realize [3] that we can approximate $m(t)$ by m_∞. Setting $\bar{a}_k = \frac{a_K}{a_{Na}}$ and $A = \frac{a_K}{c_m}$, our system finally reduces to:

$$\frac{dv}{dt} = A\left[-m_\infty^3(v)\sinh\left(\frac{q}{2kT}(v - v_{Na})\right) - \bar{a}_k w^4 \sinh\left(\frac{q}{2kT}(v - v_K)\right)\right] \tag{21}$$

$$\frac{dw}{dt} = \frac{w_\infty(v) - w}{\tau_\infty(v)} \tag{22}$$

where,

$$m_\infty(v) = \left[1 + \exp\left(\frac{z_m q}{kT}(v_m - v)\right)\right]^{-1} \tag{23}$$

$$w_\infty(v) = \left[1 + \exp\left(\frac{z_w q}{kT}(v_w - v)\right)\right]^{-1} \tag{24}$$

$$\tau_w(v) = \left[2r\cosh\left(\frac{z_w q}{2kT}(v_w - v)\right)\right]^{-1}. \tag{25}$$

In summary, the model of the neuron's membrane as a capacitor with the ion channels is being modeled by (6) and the equation for w is called first order kinetics, usually used in the literature (see for example reference [7]). The Nernst potentials for sodium and potassium are, respectively, v_{Na} and v_K. v_m and v_w are the half activation potentials for sodium and potassium respectively. T is temperature measured in Kelvins. Both Nernst potential are functions of the temperature throughout. Finally r is the rate of recovery of the potassium gate. In the equations above we see that temperature is everywhere. We are going to study this system through simulations to see how temperature affects the dynamics of the system.

Next, we provide a table of constants for the values that appear in our model:

Table 1: Physical constants and relevant parameters for the membrane potential model [6].

Constant	Value	Units	Description
q	$1.602176487 * 10^{-19}$	C	Electrical charge of one electron.
k	$1.3806504(24) * 10^{-23}$	$\frac{J}{K}$	Boltzmann constant
c_m	100	pF	Capacitance of the membrane
a_{Na}	75	nA	Amplitude of the sodium channel
a_K	14	nA	Amplitude of the potassium channel
v_w	-45	mV	Half activation potential for potassium
v_m	-30	mV	Half activation potential for sodium

3.1.2 Analysis

We will start with a study of the sodium and potassium currents and how they affect the membrane potential. We present our plots of the currents vs membrane potential in the next figure:

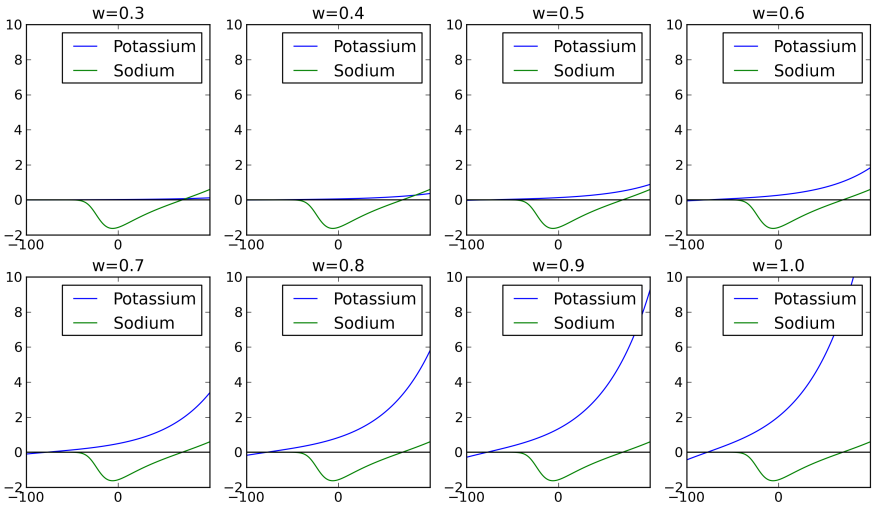

Figure 2: Current vs voltage of the potassium (blue) and sodium current (green) for different values of the gating variable w. We see that potassium current is always positive for values greater than the Nernst potential for potassium (≈ -80) and as w increase (the proportion of open channel increases) the maximum amplitude of the current increases.

To explain what is happening in this graphs we are going to see how this currents behave in three intervals:

- (∞, v_K) The potassium current is almost zero in this interval except for big values of w for which the potassium current is negative. In this interval the potassium current will increase the membrane potential according to equation (21), and that means that positive ions are going from the outside of the membrane to the inside. The sodium current is almost zero in this interval as we show in Fig. 2. Therefore in this interval the membrane potential is always increasing.

- (v_K, vNa) The potassium current is positive in this interval which means that according to equation (21) the membrane potential is decreasing which means that ions are going from inside of the cell to the outside. On the other hand the sodium current is negative which means that the membrane potential is increasing and that ions are going from outside of the cell to the inside. From this argument we can see that in this regions both currents have different effects in the membrane potential and therefore the value of the gating variable w becomes very important in determine if the membrane potential is increasing or decreasing in this section.

- (v_{Na}, ∞) In this interval both currents are positive which means that the membrane potential is always decreasing.

Another way to interpret the above observations is to think that the currents are always "pushing" the membrane potential to their respective Nernst potential.

With respect to equation (22) we can see that for every voltage v, w is going towards $w_\infty(v)$ with a velocity that is small if $\tau_\infty(v)$ is big and is big if $\tau_\infty(v)$ is small. This is why $\tau_\infty(v)$ is called relaxation time, is a measure of how much time it takes for w to arrive to a constant value for a fixed voltage. Next, we plot τ_∞ for different values of r in Fig. 3.

We can see from Fig. 3 that the more far that we are from v_m then faster the gating variable approaches to the variable $w_\infty(v)$ as v changes.

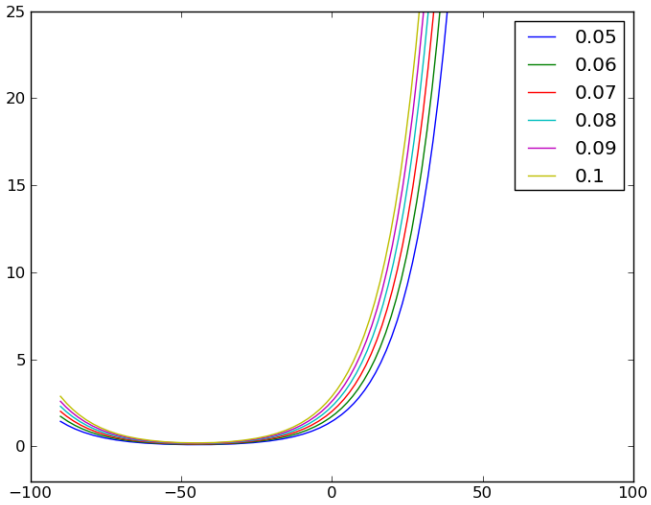

Figure 3: $\frac{1}{\tau_\infty(v)}$ for various values of r. We can see that the smaller values of r makes the curve grows slower.

3.1.3 Current clamp

We want to model how the cell is excited by an external source (for example another neuron) so in our model we would like to have a way of representing an external input. In electrophysiology the next circuit is used to have a controllable current throughout the membrane and solve that problem:

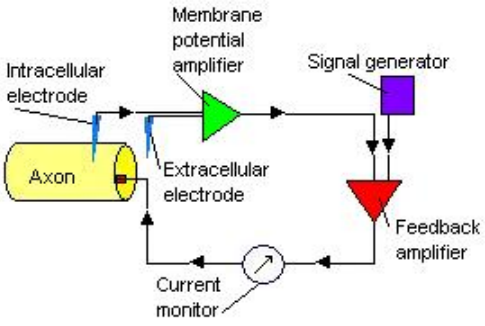

Figure 4: Current clamp circuit: Here we draw an scheme of the circuit that is used in electrophysiology to record the voltage and input a fixed current to the system

We will model that external source in our model as a square pulse, then the equation (21) becomes:

$$\frac{dv}{dt} = I + A\left[-m_\infty^3(v)\sinh\left(\frac{q}{2kT}(v-v_{Na})\right) - a_k w^4 \sinh\left(\frac{q}{2kT}(v-v_K)\right)\right]. \tag{26}$$

Our approach in this study will be to perturb the system with a square wave to see if it responds different (bifurcates) with different set of parameters for the same input.

3.1.4 Dependence on the rate of opening of potassium channels r

Time analysis

As mentioned above, the parameter r is proportional to the rate at which the gating variable w goes to w_∞. In a biophysical context it is the basal rate at which open channels close and closed channels open. According to the literature $r \in [.01, 0.1]$ (see [3], [4]). We wrote a code in python and carried out simulations of the behavior of voltage and the gating variable with those values of r and we have obtained qualitative changes on behavior (a bifurcation value) which we depict in Fig. 5.

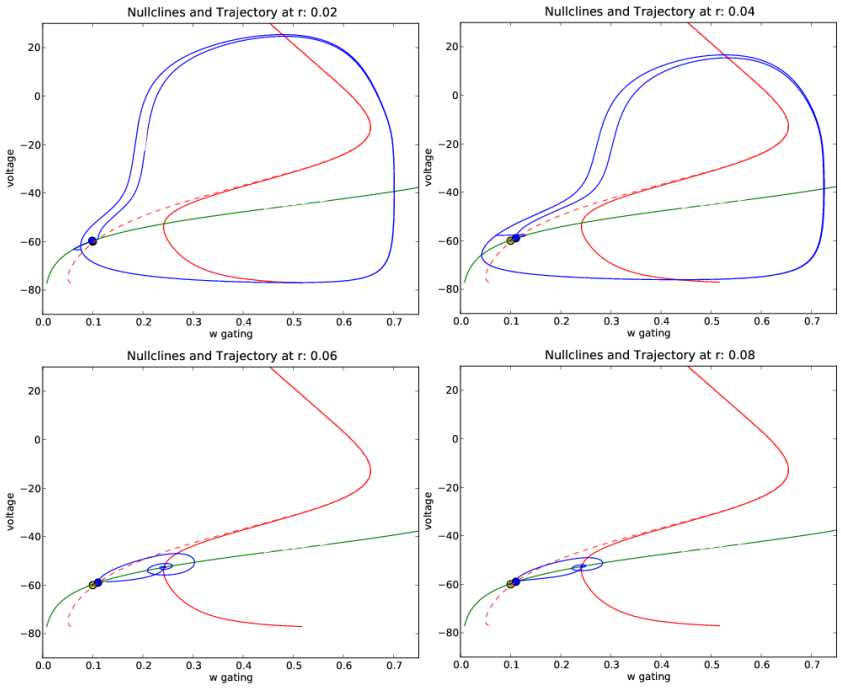

Figure 5: Temporal dynamics of v for different values of r. The figure show simulations for $r \in \{0.02, 0.04, 0.06, 0.08\}$. The numbers above indicate the value of r used for each oscillations. The temperature was 37^oC.

Here we used a square pulse I of 0.1 nano-amps from 500ms to 700ms. As we can see for the first two values of r, the trajectory spirals down to the original equilibrium point. However, for the last two values of r, the trajectory spirals out to a limit cycle. We thus observe that a small changes in r from big values to small results in a different response of the system to the same input (birth of a stable limit cycle). For w, the result is similar. We concluded that it is more feasible to have oscillations with lower values of basal rate r. We made more simulations for r and localized the bifurcation value $r*$ somewhere in $(0.047, 0.048)$.

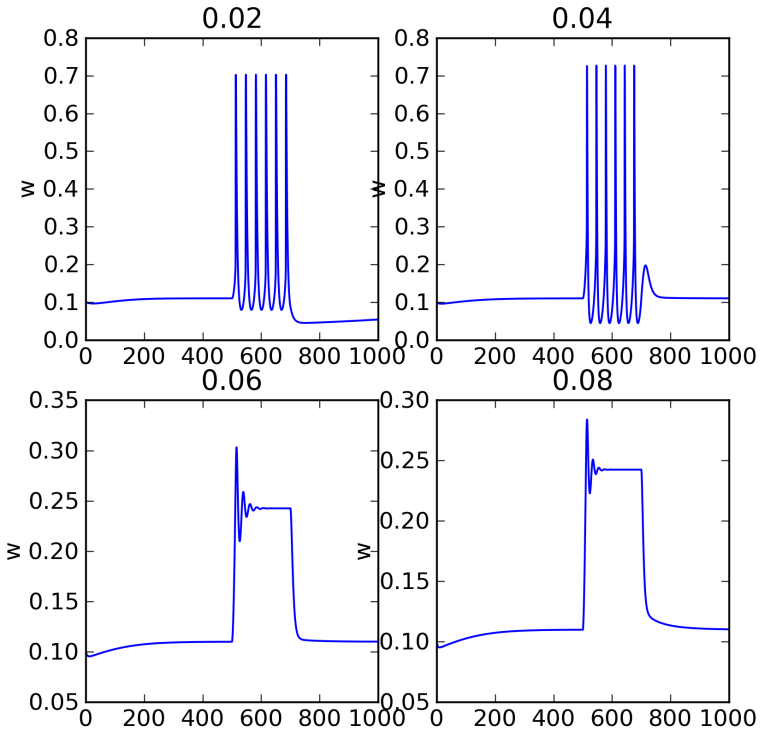

Figure 6: Temporal dynamics of w for different values of r. The numbers above indicate the value of r used for each oscillations. The temperature was 37^oC.

Phase plane analysis

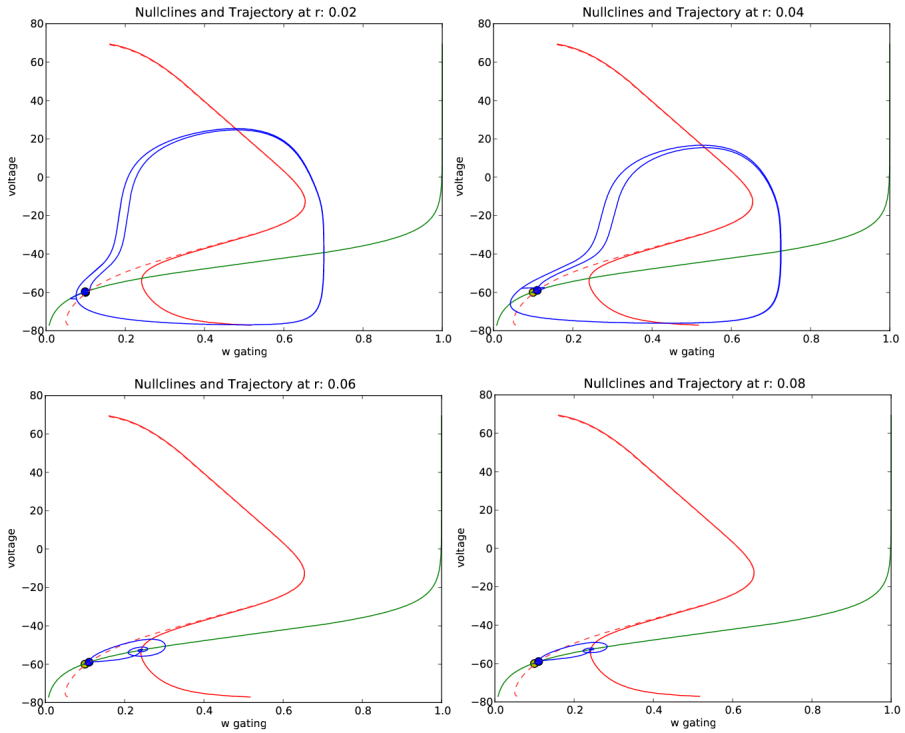

Figure 7: Bifurcation as parameter r is varied from 0.02 to 0.04. Here, $T = 37°\text{C}$. The plotting program was written in Python (see Sec. A.2 in the Appendix).

The bifurcation as r is varied while all other parameters are held fixed, including $T = 37°\text{C}$, can also be seen by examining the phase plane plots of Fig. **??**. As before, for $r = 0.02, 0.04$, the input pulse alters the location of the fixed point and changes its stability from stable to unstable, along with inducing the birth of a stable limit cycle. However, for $r = 0.06, 0.08$, the fixed point during the duration of the pulse has changed from unstable to stable, indicating the occurrence of a bifurcation between $r = 0.04$ and $r = 0.06$.

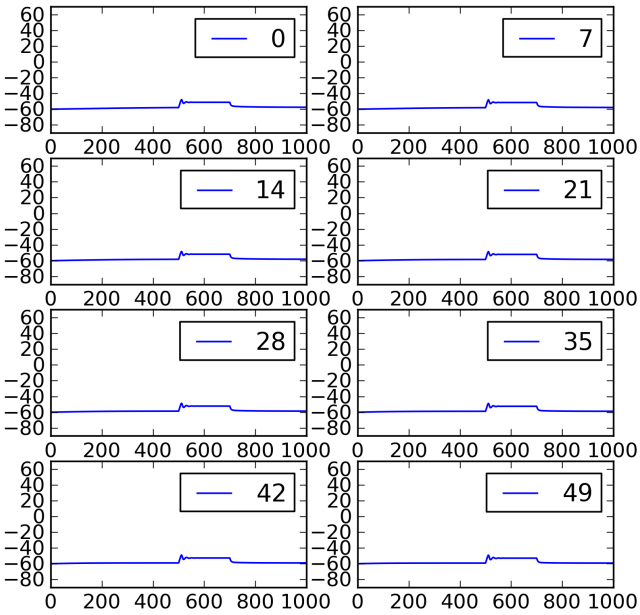

Figure 8: Membrane potential dynamics for $r = 0.08$ and different temperatures ranging from 0 to 49 degrees Celsius.

3.1.5 Analysis of the influence of temperature

Our main question in this section is how temperature affects the dynamics of the neurons' membrane. Therefore, we use some simulations in python for varying values of temperature in the range $[0, 49]$ Celsius as a parameter for different fixed values of r. First, we make some simulations for $r = 0.08$ far to the right of the bifurcation parameter $r*$ (results are show in the Fig. 8). We see that with large variation in temperature we don't get changes in the qualitative behavior of the system.

Next, we made another set of simulations with $r = 0.03$; far bigger than the bifurcation parameter $r*$ (graphs of the simulations are illustrated in Fig. **??**).

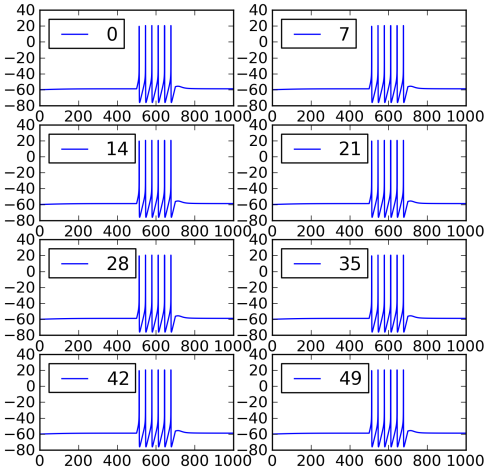

Figure 9: Membrane potential dynamics for $r = 0.03$ and different temperatures.

We can infer from this graphs that for the given change in the temperature parameter there is no change in the qualitative behavior of the system. Finally, we present in Fig. **??** the last set of simulations for $r = 0.045$ which is very near the bifurcation parameter $r*$ of the system. We see that when

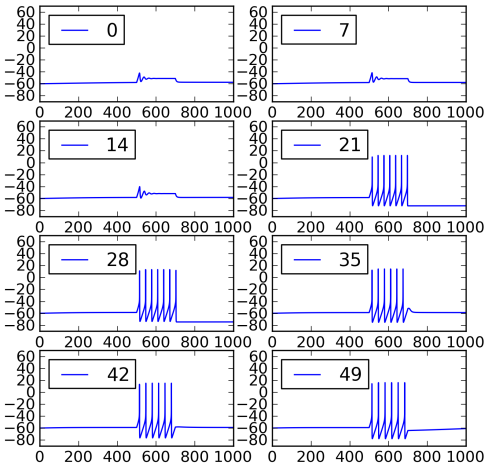

Figure 10: Membrane potential dynamics for $r = 0.045$ and different temperatures.

we are near a bifurcation value for r changes in T can induce an oscillatory behavior (a bifurcation).

Phase plane analysis

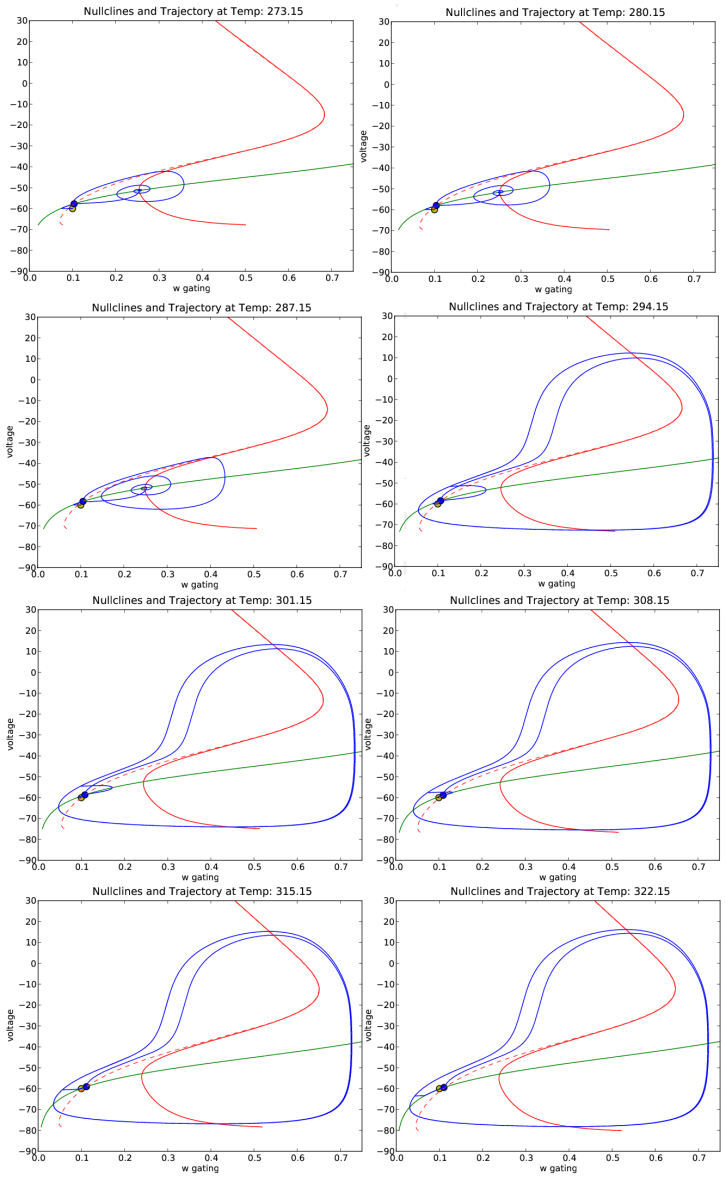

Figure 11: Bifurcation as parameter T is varied from 0°C to 49°C. Here, $r = 0.045$. The plotting program was written in Python (see Sec. A.2 in the Appendix).

Once again, phase plane plots offer another view of the bifurcation. In Fig. **??**, T is varied from 0°C to 49°C while all other parameters, including $r = 0.045$, are held fixed. Here, in contrast to the case of bifurcation due to varying r discussed above, the fixed point during the duration of the pulse is a stable one. This stability persists from $T = 0$°C to $T = 14$°C. Between $T = 14$°C and $T = 21$°C, however, a bifurcation takes place, so that the fixed point during the pulse duration becomes unstable while a stable limit cycle is born.

3.2 Application II: Dynamics of extracellular pH regulation

3.2.1 Introduction

One of the most important functions of the cellular membrane is to regulate, through channels and transporters, the concentration of the chemical species it contains. Hydrogen, (H^+), is one of the most important ions a cell embodies because it is present in many cellular processes. Nevertheless, whenever the concentration of hydrogen is outside the normal range in which a cell can properly function, the cell autoregulates itself in a process called pH regulation, a process operating in living organisms used to preserve a viable acid-base state. The pH is an expression representing the concentration of hydrogen ions and is mathematically defined by: $pH = -log[H^+]$. Depending on the physiological functionality of a biological structure a cells is part of, its internal pH values should be maintained within certain ranges [12]. Moreover, the values of pH in the extracellular environment must be kept within certain ranges because small deviations from the normal pH could disrupt the microenvironment.

Processes with major importance in pH regulation, in and outside the cell, are the buffers, chemical reactions in which hydrogen is combined with another chemical species and transform into other molecules in order to maintain certain levels of pH. When the pH is outside these ranges we say that the environment is alkaline for large values of pH, and acidic for low values.

A very interesting and remarkable case showing the effect of pH on physiology, is when cells presenting cancerous phenotypes start releasing large quantities of hydrogen into its surroundings. The reason for this pH imbalance could be a property found in most cancerous cells, that is, upregulation of glycolysis [5]. Upregulated glycolysis has as a byproduct the ion hydrogen.

This along with the fact that tumor cells have been shown to have intracellular pH similar to those in normal cells, gives rise to a high pH gradient across the cancerous cell membrane into the cellular surroundings, lowering the pH and therefore raising the acidity. On the other hand, bicarbonate is an alkaline which is a vital component of the pH buffering system of the body. In this section we intend to study the dynamics of pH levels outside the cell using a competitive-like dynamical system between the concentration of hydrogen and bicarbonate, emphasizing the role of temperature as an externally controllable parameter that could eventually be used as a therapy.

The significance of this study comes from the fact that toxic environments require the cells to evolve into phenotypes resistant to toxic environment [5]. This provokes that, eventually, cell populations with upregulated glycolysis and acid resistance mechanisms have a considerable growth advantage, which supports further proliferation and invasion of the cancerous phenotype. In fact, tumor angiogenesis, a fundamental step in the transition of tumors from a dormant to malignant state, may be regulated by pH, for it has been found that tumor cells at a low pH increase the expression of positive angiogenic factors. Moreover, it has been shown that the metastatic potential of tumor cells depends directly on the degree of acidification [5].

In this section, our study of pH regulation dynamics in the extracellular microenvironment is a first step towards a better understanding as to the biological parameters that are more important when describing the state of the system. Even though our motivation is to study the dynamics of pH regulation in cancerous cell environments, we will not explicitly include in our mathematical model any cancerous process, such as, glycolysis. In this section we focus on the process taking place in the exchangers and extracellular environment with the intention to better characterize the specificities of it. Figure 12 depicts the simplified version of the cellular environment we will model in this section.

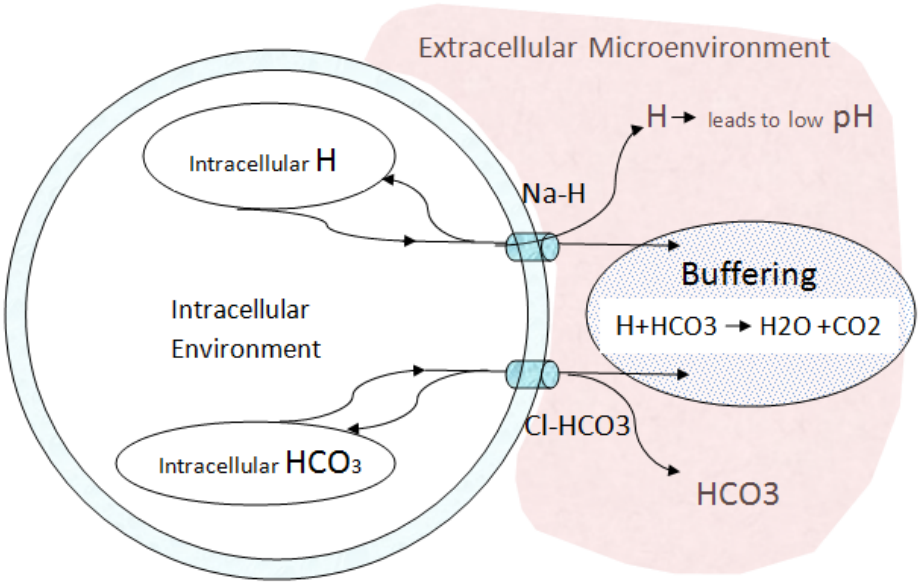

Figure 12: Description of the simplified cellular environment that will be treated in this section. Hydrogen and sodium are transported in and outside the cell through the Na^+/H^+ and Cl^-/HCO_3^- exchangers. Hydrogen ions in the extracellular environment that are not transformed in the buffering process, increase acidity.

Our approach to model pH regulation is based in part on the same thermodynamical assumptions and derivations used in the previous section. We will model the role of the membrane in this process by assuming that the hydrogen and bicarbonate ions are only transported in and outside the cell by membrane exchangers, in this case, the Na^+/H^+ and Cl^-/HCO_3^- exchangers. The other aspect of our model is the buffering process taking place outside the cell between hydrogen and bicarbonate. The rest of this section will be staged as follows. First, we present a thermodynamical derivation of the rate at which the two ions are being transported throughout the membrane. Second, we present our assumptions in the buffering process and the law we assume it is governed by. Third, we present a dynamical model for extracellular pH regulation and its stability analysis. Lastly, we study the influence of some biophysical and externally modifiable parameters in the extracellular pH value.

3.2.2 Na^+/H^+ exchanger

Of the pH regulators in the cell, the Na^+/H^+ exchanger is one of the most important. In this section, an expression for the flux of H^+ ions through this Na^+/H^+ exchanger, will be derived from a thermodynamical point of view. Contrary to the study done in the previous section, in which an electrogenic current was flowing through the Na^+/K^+ channels, this ion exchange process does not generate a net flux of charges to either side of the membrane, hence, there is no electric current. This one-to-one translocation of ions, in which one sodium ion is mechanically translocated with one hydrogen ion across the membrane, can be represented by the following reaction:

$$Na_o + H_i \rightleftharpoons_{\beta}^{\alpha} Na_i + H_o \tag{27}$$

where Na_i,Na_o, H_o and H_i are sodium and hydrogen molecules in and outside of the cell,respectively, with forward and backward reaction rates α and β.

From the Boltzmann distribution it is found that,

$$\frac{\alpha}{\beta} = \exp\left(-\frac{\triangle G}{kT}\right) \tag{28}$$

where $\triangle G$ is the Gibbs free energy of the reaction (27) [8]. The sign of the energy term determines whether or not the reaction is spontaneous. Specifically, $\triangle G < 0$ means that the reaction is spontaneous. The change in electrical potential energy due to the redistribution of charge during the reaction for a given ion σ is $\triangle G_\sigma = q(v - V_\sigma)$, where q is a gating charge ($q \approx \pm 4e$) and v is the potential difference between the two sides of the membrane, which is considered to be analogous to a two plate capacitor. For the model, V_σ is the Nernst voltage potential for the ion. In this case we have

$$\triangle G = \triangle G_H + \triangle G_{Na} \tag{29}$$

$$= -q(v - V_H) + q(v - V_{Na}) \tag{30}$$

$$= q(V_H - V_{Na}) \tag{31}$$

The V_{Na} and V_H are the Nernst potentials of sodium and hydrogen, respectively. Taking into account the explicit expression for the Nernst potential and substituting it into (31), we have

$$\triangle G = q(\frac{kT}{q} ln \frac{[H]_o}{[H]_i} - \frac{kT}{q} ln \frac{[Na]_o}{[Na]_i}) \tag{32}$$

$$= kT ln \frac{[H]_o [Na]_i}{[H]_i [Na]_o} \tag{33}$$

and substituting this result into expression (28) yields

$$\frac{\alpha}{\beta} = \frac{[H]_i[Na]_o}{[H]_o[Na]_i} \tag{34}$$

The simplest choice for α and β are

$$\alpha = \lambda[H]_i[Na]_o \tag{35}$$
$$\beta = \lambda[H]_o[Na]_i, \tag{36}$$

where λ is, in general, a function of parameters common to α and β. The net flux of hydrogen is defined as the difference between the quantity of hydrogen leaving the cell subtracting the quantity of hydrogen entering the cell, given by

$$\phi_H = \alpha - \beta \tag{37}$$
$$= \lambda([H]_i[Na]_o - [H]_o[Na]_i). \tag{38}$$

To emphasize that the two applications treated in this paper are closely related in their respective thermodynamical derivation and mathematical functionality, it is proved in the appendix that Eqn. (38) is equivalent to

$$\phi_H = \lambda\sqrt{[H]_0[Na]_0[H]_i[Na]_i}\sinh[\frac{q}{2kT}(-V_H + V_{Na})] \tag{39}$$

A similar procedure can be followed to arrive to the flux equation for HCO_3^- throughout the Cl^-/HCO_3^- exchanger.

3.2.3 Buffering process

One of the major ways in which large changes in hydrogen concentration are prevented is by buffering. This work considers the acid-bicarbonate buffer, which is chemically represented by the following chemical reaction [1].

$$HCO_3{}^- + H^+ \rightleftharpoons^1 H_2CO_3 \rightleftharpoons^2 H_20 + CO_2 \tag{40}$$

For the reaction shown above to occur, the bicarbonate ions have to come into contact with the hydrogen ions. The hydrogen and bicarbonate ions must collide at the right angle and with enough energy for the reaction to occur. Before any changes take place during the collision, the colliding molecules must have a minimum kinetic energy called the activation energy. This term

is the amount of energy needed for the reactions to approach the transition state in which bonds are broken and new bonds are formed. Heated molecules have a greater average kinetic energy, and therefore at higher temperatures, a greater number of them have the required activation energy to react. The Arrhenius Equation relates the rate of reactions and temperature as follows:

$$P(T) = a \exp\left(-\frac{E_a}{RT}\right), \tag{41}$$

where E_a is the activation energy in $Jmol^{-1}$, R is the ideal gas constant with value $8.314 Jmol^{-1}K^{-1}$ and T is the temperature in K (Kelvin). P is the rate constant that any given collision will result in a reaction per second. The total number of collisions per second leading to a reaction or not is denoted by a [1] and its units are $Lmmol/sec$. We can consider it a constant that involves chemical properties of the reactants like their concentrations and cross sectional area. The pre-exponential factor depends on temperature, but for a sufficiently small range of temperatures, its dependence on temperature is negligible compared to the effect that the temperature in the exponent has on the overall behavior of $P(T)$. By the same token, it is reasonable to approximate the activation energy E_a as being independent of temperature. It is thus observed that increasing the temperature T will result in an increase in the rate of reaction.

Although the reverse reaction ($\leftarrow$) could also take place, in this work we will not consider this case for the rate of the forward reaction ($\rightarrow$) is almost 10^4 higher than the reverse reaction [1]. In order to find the values for E_a and a it must be taken into account that the rate of reaction of the first step (1) is faster than the second step (2), so we could approximate the rate of the whole reaction as the rate of the second part, that is, the slower step. For this slower step we have several experimental results for the $P's$ and the corresponding temperatures. Notice that the Arrhenius equation could be also written as $ln(P) = -\frac{E_a}{R}(\frac{1}{T}) + ln(a)$. So if we plot different values of the pair $(P, \frac{1}{T})$, from the values of the slope and the "y" intercept we can get the corresponding values of E_a and a. These values are given below in a parameters table (Table 2).

3.2.4 Mathematical Model

Here we present a 2-dimensional competitive-like dynamical system that models the diffusion through the cell membrane and the extracellular buffer-

ing of hydrogen and bicarbonate. The system has as variables the hydrogen and bicarbonate concentrations in the extracellular environment:

$$\frac{d[H^+]_0}{dt} = N_{Na^+H^+}\lambda_1(T)\left([H^+]_i[Na^+]_o - [H^+]_o[Na^+]_i\right) - P(T)[H^+]_0[HCO_3^-]_0 \tag{42}$$

$$\frac{d[HCO_3^-]_0}{dt} = N_{Cl^-HCO_3^-}\lambda_2(T)\left([HCO_3^-]_i[Cl^-]_o - [HCO_3^-]_o[Cl^-]_i\right) - P(T)[H^+]_0[HCO_3^-]_0 \tag{43}$$

In Eqns. (42)-(43) the subscript for i and o correspond to concentrations of molecules inside and outside the cell's membrane. Because of the remarkable symmetry of the two equations, analysis of the properties of the first equation applies to the second one. In Eqn. (42) the first term is composed by a positive and negative contribution to membrane diffusion, in terms of concentrations for Na^+ and H^+ in and out of the cell. The second term represents the competitive behavior of the dynamical system, that is, the term related to the rate at which hydrogen is being transformed into H_2O and CO_2 when the buffering takes place outside the cell. It is assumed that hydrogen and bicarbonate react and "*annihilate*" one another at rate $P(T)$, given by (41). It is considered that cells have several transporters contributing to the total flux of ions. The N factor in both equations is the corresponding number of each transporter in the membrane. The parameter $\lambda(T)$ is the baseline of translocation rate and it takes the form $\lambda(T) = B/(1+e^{\theta(-T+T_h)})$. Here B, θ and T_h are constants related to the physiology of the protein that mechanically transport ions. Their values are computed so that they reflect the way we assume mammalian cell transporters behave under temperature variation. This specific functionality with respect to temperature is based on experimental facts that prove that within the range of allowed body temperature, these transporters translocate ions faster with an increase in temperature. Particularly, the values of θ and T_h are selected to fit the plausible conditions of almost no transport at $273K$ (freezing point), and maximum translocation capacity at around 313K.

Another important consideration is that the cell autoregulates itself, hence we assume that all concentrations inside the cell are held constant. Furthermore, we are also considering constant values for the concentrations of Na^+ and Cl^- inside and out the cell.

To make the previous system easier to the eye, consider $[H^+]_o = x$, $[HCO_3^-]_o = y$, $[H^+]_i = \phi$, $[HCO_3^-]_i = \beta$, $[Na^+]_{i,o} = \eta_{i,o}$, $[Cl^-]_{i,o} = \gamma_{i,o}$,

$N_{NaH} = N_1$ and $N_{ClHCO_3} = N_2$. With these redefinitions and substituting the corresponding explicit expressions for $\lambda(T)$ and $P(T)$, we obtain the following system:

$$\frac{dx}{dt} = (1/2)N_1 \frac{B_1}{1+e^{\theta_1(-T+T_h)}}(-x\eta_i + \phi\eta_0) - ae^{-\frac{E_a}{RT}}xy \tag{44}$$

$$\frac{dy}{dt} = (1/2)N_2 \frac{B_2}{1+e^{\theta_2(-T+T_h)}}(-y\gamma_i + \beta\gamma_0) - ae^{-\frac{E_a}{RT}}xy \tag{45}$$

Table 2. Parameters used in the system (44)-(45)as follows:

Parameters	Description	Value	Reference
N_1	Number of $Na^+ - H^+$ membrane transporters	500	[12]
N_2	Number of $Cl^- HCO_3$ membrane transporters	500	[12]
B_1	Physiological property	10^{-5} L/(mmol sec)	[9]
B_2	Physiological property	10^{-5} L/(mmol sec)	[9]
T_h	Temperature parameter	290 K	Estimated
Θ_1	Physiological property	0.3	Estimated
Θ_2	Physiological property	0.3	Estimated
η_i	Na^+ internal concentration	10 mmol/L	[7]
η_o	Na^+ external concentration	145 mmol/L	[7]
ϕ	H^+ internal concentration	6.3X10^{-5} mmol/L	[9]
γ_i	Cl^- internal concentration	4 mmol/L	[7]
γ_o	Cl^- external concentration	110 mmol/L	[7]
β	HCO_3^- internal concentration	24 mmol/L	[9]
a	Total number of collision per second	5.73 X 10^{10} L/(mmolsec)	[1]
E_a/R	Activation energy/R	10^4K	[1]

Rescaling of parameters

Parameter adjustments to the System (44)-(45) will be made for the sake of better handling the algebra in the following sections. Since we know the values of all the parameters, except temperature, whose manageability is the purpose of this work, we will define new parameters as a function of temperature, as follows:

$$A_{x1}(T) = \frac{N_1\eta_i}{2}\left(\frac{B_1}{1+e^{\theta_1(-T+T_h)}}\right) \tag{46}$$

$$A_{x2}(T) = \frac{N_1\eta_o\phi}{2}\left(\frac{B_1}{1+e^{\theta_1(-T+T_h)}}\right) \tag{47}$$

$$A_{y1}(T) = \frac{N_2\gamma_i}{2}\left(\frac{B_2}{1+e^{\theta_2(-T+T_h)}}\right) \tag{48}$$

$$A_{y2}(T) = \frac{N_2\gamma_o\beta}{2}\left(\frac{B_2}{1+e^{\theta_2(-T+T_h)}}\right) \tag{49}$$

Notice that all these new parameters are positive. The biological significance of these parameters is as follows:

- $A_{x1}(T)$ represents the rate at which H^+ is entering the cell due to the number of Na^+H^+ channels, rate of transport and Na^+ internal concentration.
- $A_{x2}(T)$ represents the rate at which H^+ is being pumped out of the cell due to the number of Na^+H^+ channels, rate of transport, Na^+ concentration outside and inside H^+ concentration.
- $A_{y1}(T)$ represents the rate at which HCO_3^- is entering the cell due to the number of $Cl^-HCO_3^-$ channels, rate of transport and Cl^- concentration inside.
- $A_{y2}(T)$ represents the rate at which HCO_3^- is pumped out of the cell due to the number of $Cl^-HCO_3^-$ channels, rate of transport, Cl^- concentration inside and HCO_3^- concentration inside.

With the changes done in (46)-(49) our new system is now

$$\frac{dx}{dt} = -A_{x1}x + A_{x2} - Pxy \tag{50}$$

$$\frac{dy}{dt} = -A_{y1}y + A_{y2} - Pxy. \tag{51}$$

3.2.5 Stability analysis

Newtonian equivalent

In this section we propose a mechanistic approach to qualitatively describe the previous system [10]. If we substitute (51) into (50) we will obtain the following equation for $x(t)$

$$\frac{d^2x}{dt^2} = \left(-\frac{A_{x2}}{x}\right)\frac{dx}{dt} - [(xA_{x1} - A_{x2})A_{y1} + Px(A_{y2} + xA_{x1} - A_{x2})] \tag{52}$$

where the variable $x(t)$ could be considered as the position of a particle under the influence of a non-conservative force and a conservative force field whose potential $V(x)$ is given by

$$a(t) = F_{non-cons}(x, dx/dt) + F_{cons}(x) \tag{53}$$

$$F_{cons}(x) = -\frac{dV}{dx}. \tag{54}$$

Integrating the conservative force we obtain for the potential the following expression

$$V(x) = \frac{PA_{x1}}{3}x^3 + (A_{y1}A_{x1} + PA_{y2} - PA_{x2})\frac{x^2}{2} - A_{y1}A_{x2}x. \qquad (55)$$

Knowing the graphical properties of this potential we can perform a qualitative analysis of the system in terms of the variable x, i.e., $[H^+]_o$. Depending on the initial position x_o, the motion of the particle over time will depend on the shape of the potential within the vicinity of x_o. This initial condition is physically equivalent to the total energy the particle has, that is, $E_t(0) = V(x_o)$. If there are no driving forces and we trace a horizontal line $E_t(0) = V$, characterizing the total energy of the system E_t, this line will delimit the permissible ranges of motion of the particle. The role played by the non-conservative force depends on the sign of the factor multiplying the velocity term dx/dt. Inspecting Eqn. (55) it is clear that this term is always negative, therefore this force will dampen the motion of the particle at all times. However, it is interesting that the absolute value of this term $-A_{x2}/x$ is inversely proportional with x. This damping force becomes larger the smaller the value of the variable. This could mean that when the hydrogen concentration declining, the corresponding Na^+/H^+ exchanger regulates the incoming gradient of hydrogen by impeding it. For large values of x, the force is still dampening the motion but the influence is less relevant. For this later case, we could think that the only force acting on the system is the conservative one, and the shape of the potential in that vicinity will almost totally dictate the dynamics of the system.

For all positive values of the parameters defined in Eqs. (46)-(49), it can be analytically proved that this potential will have three zeros, one at the origin and the other two on opposite sides of the origin. It also has two local extremes at different sides of the axes $x = 0$, a maximum to the left, and a minimum to the right. Thus, for positive values of x, the potential behaves as a concave up parabola with the minimum under the $V(x) = 0$ axes. For our purposes, only positive values of the variable x are of interest. This minimum represents then, the only stable point of the system, and so it is globally stable. The analytical prove of these characteristics of $V(x)$ are in the appendix.

Now that the shape of the potential is clear, let's analyze again the role of the dissipative force $-A_{x2}/x$, which is quite relevant in the system. Using the potential analogy, it can be said that the body is moving under friction-

like conditions, and given any initial conditions it will tend to approach the minimum. Once it reaches it, the effect of an increasing slope to overcome, plus a resistive "medium", makes the particle stay near the minimum, until it finally reaches it. This behavior is equivalent to a stable node in dynamical systems theory. Biologically this means that, for fixed parameters' values, the $[H^+]_o$ always reaches the same equilibrium value, and so does the pH.

Dynamical systems approach

If we find the general determinant and trace of the Jacobian of System (50)-(51), we obtain

$$D(x,y) = A_{x1}A_{y1} + P(xA_{x1} + yA_{y1}) \quad (56)$$
$$Tr(x,y) = -A_{x1} - A_{y1} - P(x+y). \quad (57)$$

From the expression in Eqn. (56) we notice that $\forall_{(x>0,y>0)} : D(x,y) > 0$. Notice that the variables are concentrations of molecules, hence negative values of these variables are not biologically significant. Therefore, the previous condition will hold true for the interest of this work. For this reason we can already predict that none of the equilibrium points will be characterized as a saddle point. From the trace we can also tell that this fixed point will be stable because this trace is negative $\forall_{(x>0,y>0)}$. To this point we know that if the two fixed points of the system in Eqs. (50)-(51) belong to the first quadrant, then two of the possible stability description are: two stable equilibrium points or a limit cycle. Next, we will prove that none of these possibilities are allowable, leaving us with the case of only one locally asymptotically stable point in the first quadrant, and the other fixed point will geometrically fall in a range that makes it negligible for our purposes.

Dulac's criterion

Dulac's criterion [11] provides us with a formal proof to rule out the possibility of closed orbits, considering that limit cycles are particular cases of closed orbits. The criterion is stated as follows: let $\dot{\mathbf{x}}$=$\mathbf{f}(\mathbf{x})$ be a continuously differentiable vector field defined on a simply connected subset R of a plane. If there exists a continuous differentiable, real-valued function g($\mathbf{x}$) such that $\nabla \cdot (g\dot{\mathbf{x}})$ has one sign throughout R, then there are no closed orbits lying entirely in R.

In our case $\dot{\mathbf{x}} = (dx/dt, dy/dt)$, our R subset is $\Re^{2+}$ and we can select g($\mathbf{x}$)=1. We have then

$$\nabla \cdot (g\dot{\mathbf{x}}) = \nabla \cdot (\dot{\mathbf{x}})$$
$$= \frac{\partial(-A_{x1}x + A_{x2} - Pxy)}{\partial x} + \frac{\partial(-A_{y1}y + A_{y2} - Pxy)}{\partial y} \quad (58)$$
$$= -A_{x1} - A_{y1} - P(x + y) \quad (59)$$

The last result is the trace found in Eqn. (57), which will always be negative for all values of the $\Re^{2+}$ subset. With this, it can be guaranteed that no limit cycles will exist in the system.

To address the possibility of two stable points within the $(\Re^2)^+$ subset, it is considered that each point is surrounded by a domain of attraction which are open sets Γ_1 and Γ_2, which implies that the set $^{\neg}(\Gamma_1 \bigcup \Gamma_2) = \Omega \neq \emptyset$. Therefore, it could be encountered a contradictory situation in which if the system is in a point $(x, y) : (x, y) \in \Omega$, then the point has no attractor and this is not possible, for the point will behave as a fixed point, and we already know that the system only has two fixed points. In a more general case we could have a whole set of points described by the curve $\zeta \in \Omega$ that behaves like if it has an attractor of its own, which is also contradictory because we only have two attractors.

Considering that only one point is allowed on the $\Re^{2+}$ subset, we will not have the case of an initial condition outside the interesting range leading to a solution curve that enters the the first quadrant, and viceversa. That is assured because no point starting on the biologically plausible range will exit this range. This can be proved by setting $x = 0$ and $y = 0$ in the system (50)-(51):

$$\frac{dx}{dt} = A_{x2} > 0 \quad (60)$$

$$\frac{dy}{dt} = A_{y2} > 0. \quad (61)$$

These expressions mean that if the system is at any pair $(x > 0, y > 0)$ near any of the axes, the dynamics tends to "push" the system away from the edges, hence the curve that describes any solution will never exit the first quadrant.

Ruling out spiral stability

We are left with two options to describe the stability of the system, i.e., stable spiral or stable node. In this section we will provide a condition that rules out the possibility of spirals. The values of the eigenvalues of the system (50)-(51) are given by:

$$\rho_{1,2} = \frac{1}{2}(Tr(x,y) \pm \sqrt{Tr^2(x,y) - 4D(x,y)}) \tag{62}$$

To prove that there are no spirals, we must have that the eigenvalues have no imaginary part, and this is given by analyzing the sign of the expression $Tr^2(x,y) - 4D(x,y)$. In fact, if $Tr^2(x,y) - 4D(x,y) > 0$ it can be assured that there will be no spirals. Algebraically working with Eqn. (56) and (57) we obtain:

$$Tr^2(x,y) - 4D(x,y) = (A_{x1} - A_{y1})^2 + P^2(y+x)^2 + 2P(y-x)(A_{x1} - A_{y1}) \tag{63}$$

Considering that biologically it is sound to say that $y >> x$ at all times (because $[HCO_3] \approx 10^6[H]$ in the extracellular fluid [9]), we could say that is a good approximation to propose that $(y \pm x) \approx y$. Using that result in (63) we obtain:

$$Tr^2(x,y) - 4D(x,y) = (A_{x1} - A_{y1})^2 + P^2(y)^2 + 2P(y)(A_{x1} - A_{y1}) \tag{64}$$

$$= ((A_{x1} - A_{y1}) + Py)^2 \tag{65}$$

which will never be less than zero, and therefore we will not have imaginary eigenvalues. Therefore, we will not have spirals and our stable point will always be a locally asymptotically stable node in the $\Re^{2^+}$ subspace.

If the value of hydrogen concentration always tends to a stable node, then the pH value should have the same behavior. In Fig. 13, we present the graphs of numerical solutions of pH vs t for different initial conditions of pH. It is clear how all the solutions tend to the same asymptotic value of pH, in agreement with the analytical results found above.

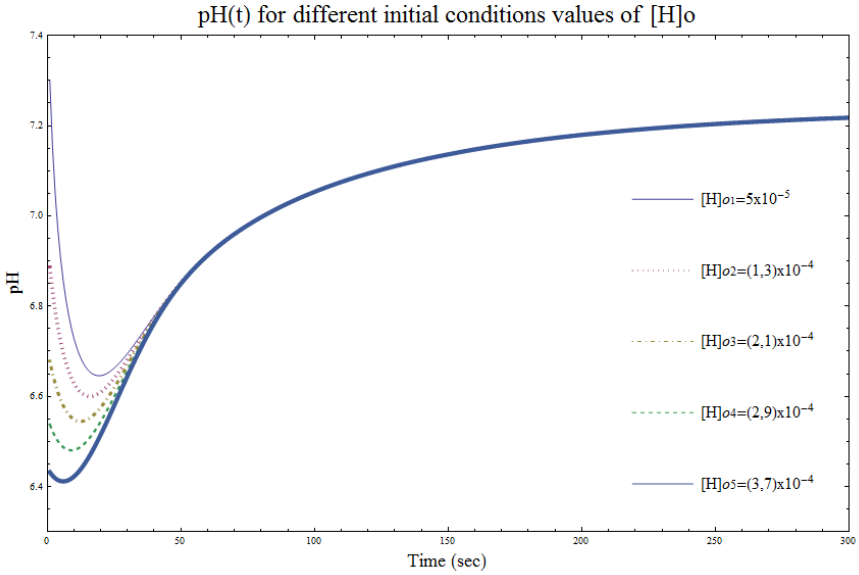

Figure 13: pH(t) for different values of $[H]_o$ in mmol/L. All initial conditions tend to the same pH value.

3.2.6 Stable point variation with temperature and other parameters.

Now that we know of the sole existence of a stable point on $\Re^{2+}$, we want to explore its coordinate dependence with temperature and other parameters. The idea is to explore how this stable point, which characterizes the steady state of the biological system in the extracellular microenvironment, i.e., its pH_e, given the fact that $pH_e = -\log([H_o])$, moves around the phase plane when the parameters of the system are modified. Special emphasis is made on the role of the parameters θ_1 and T_h, for they describe the behavior of the transporter as a function of temperature, i.e., the diffusion dependence with temperature of the membrane flux of ions. Next, we present several graphs which have been computed using the parameter values in Table 2.

Fig. 14 shows a plot of pH vs. T for various values of the computed parameter T_h. We took values of these parameters in a range around the selected value $290K$. Notice that the curves $pH(T)$ have a local minimum that moves to the left as T_h increases. Moreover, the T value of these minimum are very close to the corresponding T_h. Mathematically this means that

depending of the value of T_h, the slope of the curve will shift at that value of temperature. This behavior is remarkably related to the shape of $\lambda_1(T)$ which dictates the rate of flux of the transporter depending on temperature. In terms of the biological matter, the dependence of pH with temperature depends on what ranges of temperatures are being considered. If we assume that the value of $T_h = 290K$ is biologically sound, and considering that a human body temperatures are normally inside the range $[303 - 315K]$, we can say that for most human body purposes, pH is a crescent function of temperature. This result has been shown experimentally in a study made of pH dependence with temperature in guinea-pig ventricular myocytes [2]. In one of their results they show how when varying the temperature from $310K$ to $300K$ the pH drops from around 7.3 to 6.8. This is numerically reflected on Fig. 14 for parameter values in the range $T_h \leqq 290$. Another interesting feature is that for $T = T_h \Rightarrow \lambda(T = T_h) = B/2$ which means that the level of acidity is greater when the transporter is transporting at half its maximum capacity.

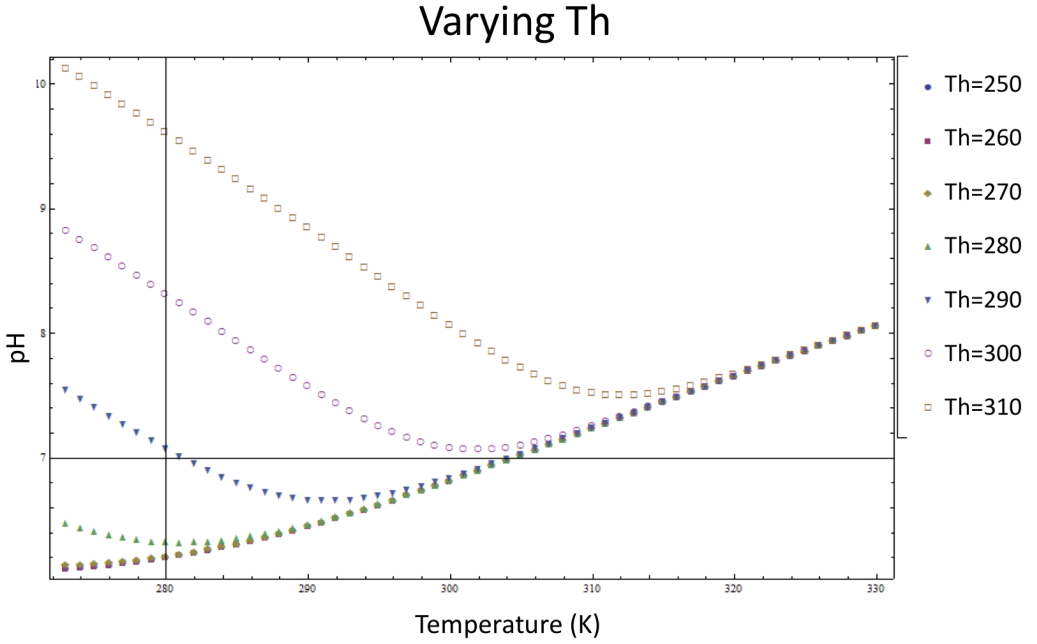

Figure 14: pH(T) for different values of T_h. The maximum acidity is reached when $T = T_h$.

In Fig. 15 we again plot pH vs. T, this time varying the exponential factor θ_1. Here $T_h = 290K$. Notice that the lower the value of this parameter, the lower the slope of the graph for $T < T_h$. The dependence does not change significantly for values of pH($T > T_h$). Analyzing the mathematical definition of $\lambda_1(T)$ we notice that the effect of the exponent $(-T+T_h)$ is less important as θ_1 decreases. Actually, for sufficiently small values of θ_1, the temperature dependence of $\lambda_1(T)$ vanishes and at the limit we have $\lambda_1(T) = \frac{B_1}{2}$, in which case we have a flux of ions through this transporter that would only depend on rates of concentrations of ions in and out of the cell. We will not consider this perspective valid in this paper, but it is still interesting to see that pH(T) is almost monotonously increasing when the transporter behavior does not depend on temperature.

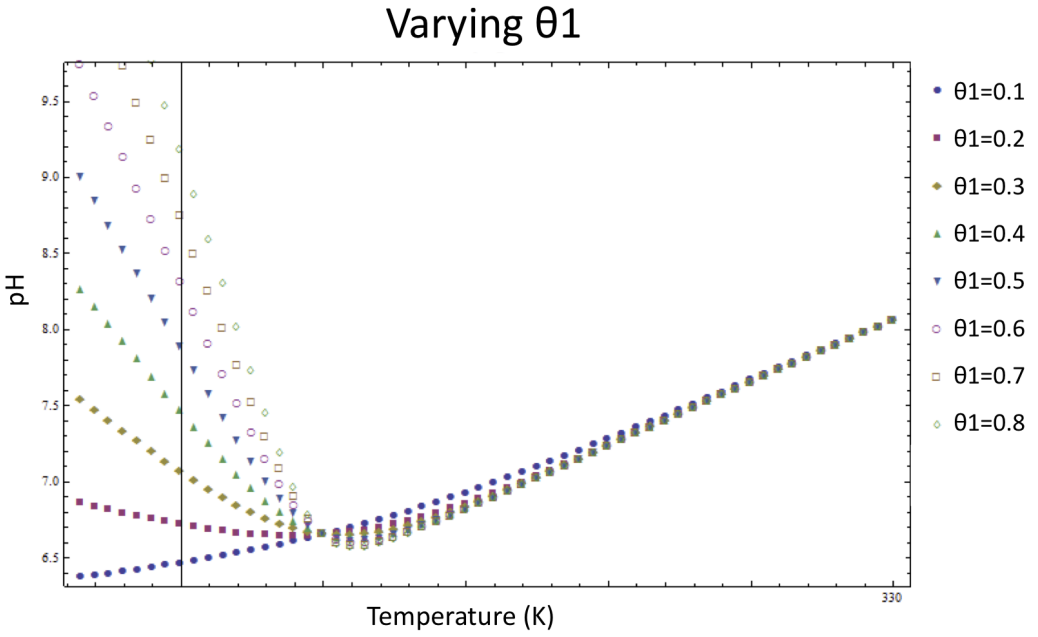

Figure 15: pH(T) for different values of θ_1

Fig. 16 is a plot of pH(T) vs. T for various values of the parameter $r = N_1/N_2$. By inspection is clear that increasing the value of r will only displace the graphs downward. This is an intuitive result considering if the number of Na^+/H^+ transporters is increasing, then more hydrogen is being pumped out of the cell, therefore, the lower the extracellular value of pH.

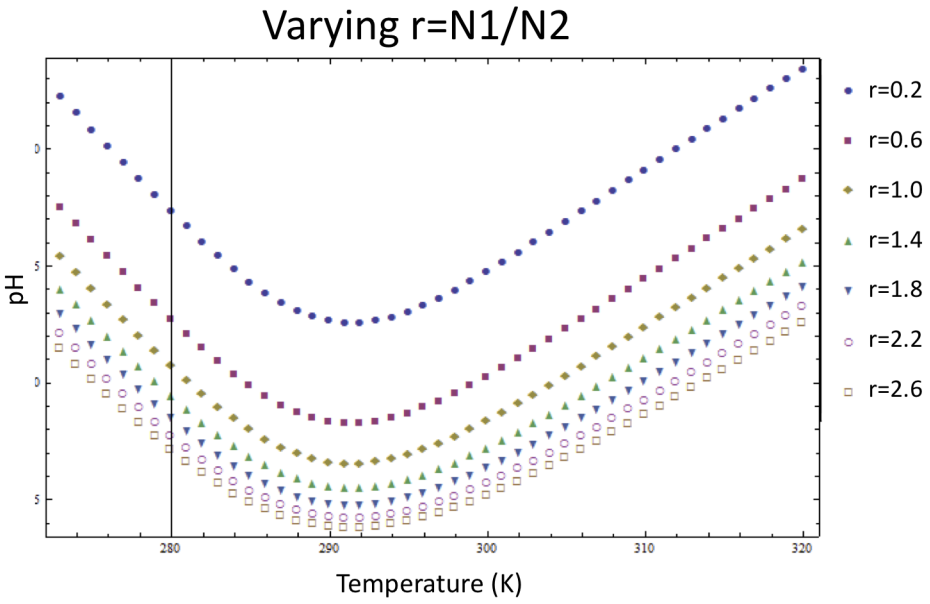

Figure 16: pH(T) for different values of r. Increasing the value of N_1 makes the extracellular environment more acidic.

Another interesting feature to notice is that the difference in the pH values for two successive values of r diminishes as r grows. For relatively large values of r the graphs tend to superpose. Therefore, there is a certain value of N_1, given that N_2 is kept constant, after which the net effect that has on the extracellular pH is not as relevant as when $N_1 \lesssim N_2$. This could be biologically interpreted as the situation when there is relatively a low number of Na^+/H^+ transporters, all of the flux of hydrogen is ejected to the extracellular space which increases the pH. However,as the number of exchangers increase the concentration of hydrogen also increases which results in having some of the ions re-entering the cell by diffusion. In the limit case of $N_1 \gg N_2$, a self- attained, low pH equilibrium is reached by the Na^+/H^+ transporter which now dictates most of the dynamics of the whole pH regulation system.

Increasing the activation energy moves the graphs downward as well, (see Fig. 17). This is another intuitive result that stems from considering a Maxwell Boltzmann probability distribution [1] as a fair characterization of the energy of the system of hydrogen ions that are possible reactants of

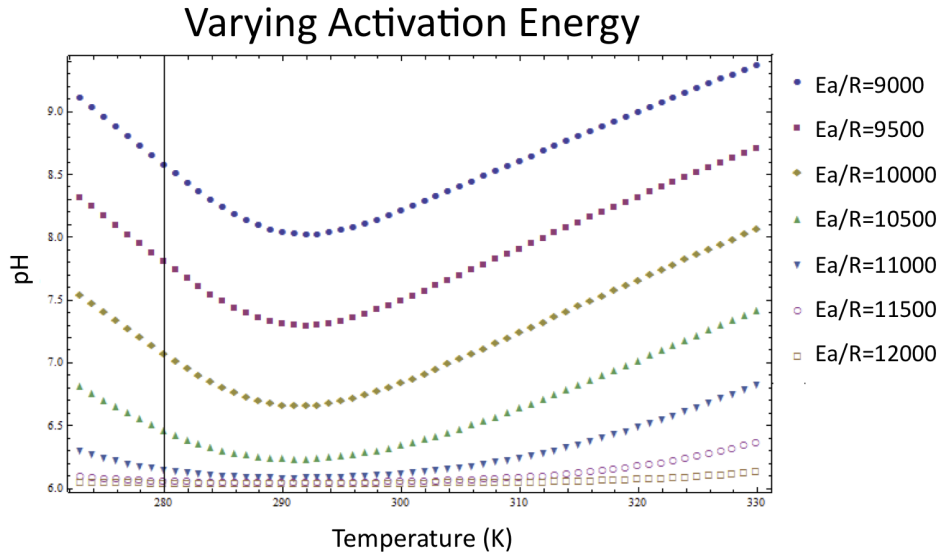

Figure 17: pH(T) for different values of E_a. For higher values of E_a the levels of acidity increase.

the buffering reaction. As the activation energy increases, ions decrease the chance of surpassing this activation energy. Therefore, fewer hydrogen ions will react and transform into other chemical species. The final outcome is that a higher $[H]_o$ will result in a lower extracellular pH.

Aside from the displacement effect, increasing E_a has another remarkable feature: the graph expands as E_a grows, making $pH(T)$ have a relatively small positive slope. A biological interpretation for this is that when the activation energy reaches a certain threshold value, the buffering process will not take place and hydrogen ions will not have enough energy to react. Therefore, the dynamical process is dictated by the transporters, and the resulting uncoupled system will be

$$\frac{dx}{dt} = -A_{x1}x + A_{x2} \tag{66}$$

$$\frac{dy}{dt} = -A_{y1}y + A_{y2} \tag{67}$$

with trace and determinant given by

$$D'(x,y) = A_{x1}A_{y1} \quad (68)$$
$$Tr'(x,y) = -A_{x1} - A_{y1} \quad (69)$$

and a stable point uniquely given by $(\frac{A_{x2}}{A_{x1}}, \frac{A_{x2}}{A_{y1}})$, which can be proved to be a stable node from the values of D' and Tr'. This means that each transporter on its own will reach an equilibrium state for any given set of parameter values. In this case, it would be plausible to introduce the temperature dependence of the pre-exponential factor a of the Arrhenius equation. This factor includes properties of the system regarding the spatial configuration, and more importantly, the kinetic energy of the ions as a function of temperature. More specifically, its dependence is $a(T) \sim \sqrt{T}$. With this factor included, the energy of the ions would raise with temperature and would have a greater chance to overcome the reaction barrier imposed by a high value of E_a. Under these considerations, the buffering process would still have to be considered.

3.2.7 Sensitivity analysis of the pH(t) with respect to parameters

In this section we study the sensitivity of pH over time with respect to some of the parameters of the system. In particular we selected temperature (T) and the same parameters studied in the previous section, namely, T_h, θ_1, N_1 and E_a. The reason why we make such an emphasis in studying the behavior of our system in relation to these parameters is because their exact values have not been experimentally found or they can vary from cell to cell. In the case of T, N_1 and E_a we also have the opportunity to modify them as an exterior influence over the system. Before showing our results, we present the numerical procedure followed to obtain them. From the sensitivity analysis theory it is known that the definition of the sensitivity index S of a function $\chi(t,p)$ of parameter p is given by

$$S_p(\chi(t)) = \frac{\frac{\delta\chi}{\chi}}{\frac{\delta p}{p}} = \frac{\partial\chi}{\partial p}\frac{p}{\chi}. \quad (70)$$

This index gives us an idea of what percentage change will produce in the function $\chi(t,p)$ a given percentage change in the parameter p. In this work, a numerical approximation of this problem was made. Given a parameter p_i we wanted to study, a numerical solution of the system (50)-(51) was obtained

for two close values of the parameter p_i^1 and p_i^2, such that $p_i^2 - p_i^1 = 0.01 p_i^1$, i.e., we varied the parameter by 1%. Only the solutions $x_{p_i^1}(t)$ and $x_{p_i^2}(t)$ are taken into consideration because the value of pH is given by $pH(x) = -Log(x)$. Then we define as our sensitivity index $S_{p_i}(x(t))$ as

$$S_{p_i}(x(t)) = \frac{x_{p_i^2}(t) - x_{p_i^1}(t)}{p_i^2 - p_i^1} \frac{p_i^1}{x_{p_i^1}(t)} \tag{71}$$

and for the pH

$$S_{p_i}(pH(t)) = \frac{pH_{p_i^2}(t) - pH_{p_i^1}(t)}{p_i^2 - p_i^1} \frac{p_i^1}{pH_{p_i^1}(t)}. \tag{72}$$

The graphs of the different sensitivity indexes for all the previously mentioned parameters are plotted in Fig. 18 .

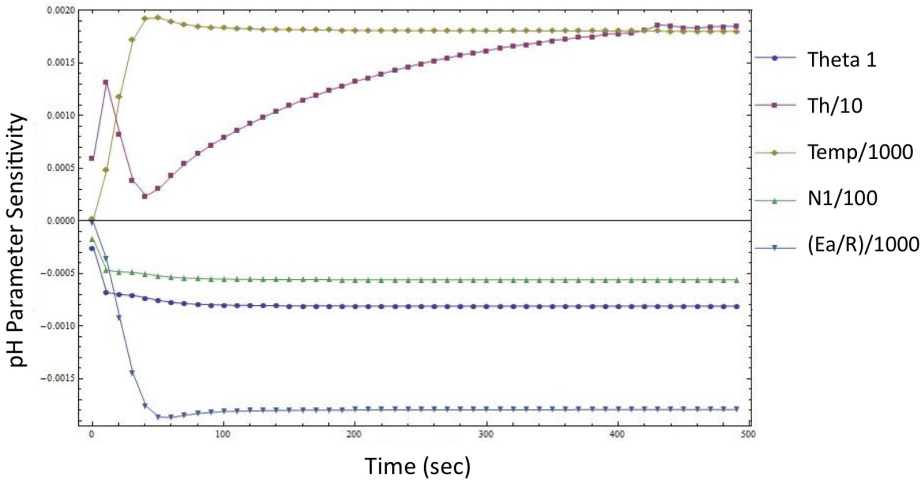

Figure 18: Sensitivity of pH(t) with respect to parameters

At this point, it is important to remark that the sensitivity analysis is the study of the relative effect that has on the system perturbing the parameter value within a small vicinity of this value. We could then consider a five-dimensional parameter space. The position of a point in this hyperspace partially describes the physiology of the process of pH regulation outside the cell. As long as this sensitivity analysis is a local study of the parameter-dependence of the system, it is necessary to define a point that locates the

position we suppose best describes our system. For that matter, it is assumed that in standard conditions, this extracellular environment would be described by a point P_o given by

$$P_o = (T, T_h, \theta 1, N_1, \frac{E_a}{R}) = (310K, 290K, 0.3, 500, 10^4 K) \tag{73}$$

Our analysis will discriminate which parameters have greater effect on the system when perturbing these quantities by a small amount from P_o.

A significant feature to notice in this figure is that the graphs of some of the parameters have been rescaled to make them fit in the same plot. Specifically, T and E_a were rescaled to $1/1000$ of their original index values, whereas N_1 and T_h were rescaled to $1/100$ and $1/10$, respectively. This means that parameters like T and E_a have a great sensitivity index compared to other ones because slightly varying their values would significantly change the final pH value. From this graph is also clear the effect that augmenting each parameter will have on the pH behavior. In this respect, the effect of each parameter seen in Fig. 18 is correspondent to the conclusions arrived at in the previous section. For instance, a small increment in temperature from the value 310 K, will cause the pH to raise. Conversely, an increment in E_a will cause the pH to drop. For the case of θ_1 and T_h we can say that their impact on the system is not as crucial as the other three parameters. This is a relevant result because these two parameters reflect the physiological properties of the transporter. Hence, these low sensitivity indexes suggest that perturbing the particular properties of each transporter from point P_o will not have a significant impact on the pH regulation process.

From a more general perspective, we could divide our graph into three time regions that present different overall behaviors. We would then have $\tau_1 = (0, \sim 10sec)$, $\tau_2 = (\sim 10, \sim 50sec)$ and $\tau_3 = (\sim 50, 500sec)$. In τ_1 we have that all indexes functions are increasing in absolute value with respect to time, so their influence in the system is greater with time. Around $t \approx 10sec$, $S_{\theta_1}(pH(t))$ and $S_{N_1}(pH(t))$ reach an asymptotically stable value, and $S_{T_h}(pH(t))$ changes its rate of growth form positive to negative. Around $t \approx 50sec$ we have that $S_{E_a}(pH(t))$ and $S_T(pH(t))$ reach their maximum and lower their indexes in absolute value until they reach a stable value, whereas $S_{T_h}(pH(t))$ again switches its rate to positive and slowly increases its sensitivity index values until it also reaches an asymptotically stable value. If we consider that the system has been running for a long enough time we could consider only the steady state value of the respective indexes and

conclude that T and E_a have the greatest impact on the system. This result confirms our initial assumption that temperature is a fundamental factor in regulating pH.

4 Discussion

In Sec. 3.1 we presented a biophysical model of a neuron that, for some combinations of parameters, displays sustained oscillations for a range of temperatures. Our model is composed of two nonlinear equations, one for describing the change of voltage through the membrane, and other for describing the dynamics of the potassium gate. Our primary purpose was to see how temperature affects that system because this physical variable is typically assumed to be constant in excitable cell studies. In order to do this first we studied how were the variations of the system with respect to the rate of recovery of the potassium variable r. Our results showed that we can obtain oscillations for small values of r and excitability for big values of r. After that we have studied how the system behaves with different values of the temperature for fixed values of r. Our simulations show that transitions between oscillatory and non-oscillatory behavior occur as a function of T depending on the parameter r.

Using a thermodynamical approach we explored the dynamics of the pH regulation process in the extracellular environment. We found that the dynamical system describing the process has only one equilibrium point and its stability is always that of a globally stable point. This means that, for all initial conditions of hydrogen concentrations, the system will always tend to the same stable node, given that the biological parameters are kept fixed. We took advantage of this rather simple dynamical behavior to thoroughly investigate the sensitivity indexes of the system with respect to parameters of interest, such as T, T_h, θ_1, N_1 and E_a. It was determined that the pH regulation process is greatly influenced by small changes in T and E_a, agreeing with our initial prediction that temperature played a significant role in the system. Furthermore, assuming certain values of estimated physiological parameters, we found that, in ranges of normal body, pH and temperature are proportional. It was also concluded that the parameters describing the Na^+/H^+ transporter, i.e., θ_1 and T_h, if selected in certain ranges, they could drastically change the dependence of temperature with pH.

With the use of a simplified version of cellular environment, we gained

a better understanding of the dynamics of pH regulation. With this knowledge, we intended to manage the geometric position of the phase plane point describing the biological state of the system, in particular $[H]_o$, such that it lies within a range of normal extracellular pH conditions that are favorable for normal cells. In particular, we aim at keeping the system out of ranges of low pH, where toxicity can be extremely dangerous for normal cells and very advantageous for tumor cells to spread their domain and become large enough to provoke angiogenesis and metastasis. With this objective, we explored the influences of temperature and other thermodynamic parameters in the transport of ions across the cell membrane and the buffering of hydrogen in the extracellular environment. Starting from the initial condition of a toxic environment, i.e., a low pH, we intended to change the stable point position of the system by manipulating a set of modifiable parameters, that is, $r = N_1/N_2$, E_a and T. For the case of r, if we started in a low pH environment, we saw from the graphs in Fig. 16 that decreasing the value of r will raise the pH value. This could be done by utilizing transport inhibitor proteins which decrease the transport capacity of the membrane, i.e., its ability to acidify the environment. There are many Na^+/H^+ exchangers across the membrane that play important roles in intracellular pH regulation. Under inhibition by enzymes, such as protein kinase A, the Na^+/H^+ exchanger could decrease the expelling of hydrogen which would increase the pH extracellularly.

For the case of the activation energy, it is found that lowering its value notably augments the pH values. This could be achieved with the help of specific catalytic enzymes. In general, catalysts are substances that increase the rate of chemical reactions by introducing alternative pathways for reactions to occur, thus decreasing activation energy. Carbonic anhydrase is the enzyme that catalyzes the reversible reaction between carbon dioxide hydration and bicarbonate dehydration, which includes the reaction between hydrogen and bicarbonate. Under high pH, the active site for this enzyme reacts on the hydration of carbon dioxide and under low pH, reacts on the dehydration of bicarbonate. Thus, the pH can be better regulated by the buffering between bicarbonate and hydrogen with the carbonic anhydrase enzyme.

4.1 Future work

In a subsequent job we are aiming to study the feasibility of using T as a bursting parameter. In future work we will consider the explicit temperature dependence of the pre-exponential factor on the Arrhenius equation, a. Also, we shall consider removal of hydrogen by introducing a vascular parameter, since we are assuming that all the hydrogen that leaves the cell, either returns into the cell by diffusion or remains near the cell in a microenvironment. This would open doors to an explicitly expressed glycolytic process inside the cell as time dependent producer of hydrogen, to enhance the study of the cancer cell and what parameters play the more significant role when preventing further spread of this phenotype.

Acknowledgments

This project has been supported by grants from the National Science Foundation (NSF - Grant DMPS-0838705), the National Security Agency (NSA - Grant H98230-09-1-0104), the Alfred P. Sloan Foundation; and the President and Provost Offices at Arizona State University. The Mathematical and Theoretical Biology Institute now hosted at the Mathematical, Computational and Modeling Science Center at ASU would like to give thanks to everybody involve with the program for the past 15 years. We thank Benjamin Morin, José Vega, Dr. José Flores, and Dr. Leon Arriola for their valuable help in constructing our work. We would also like to thank Dr. Carlos Castillo-Chavez for providing us with the great opportunity of being participants of MTBI 2010.

References

[1] Theodore L. Brown, H. Eugene LeMay Jr., Bruce E. Burnsten, and Catherine J. Murphy. *Chemistry The Central Science*. Pearson Prentice Hall, Upper Saddle River, NJ 07458, fifth edition, 2009.

[2] Frederick F. T. Ch'en, Emma Dilworth, Pawel Swietach, Ruch S. Goddard, and Richard D. Vaughan-Jones. Temperature dependence of $na^{+}-h^{+}$ exchange, $na^{+}-hco^{-}\_3$ co-transport , intracellular buffering

and intracellular ph in guinea-pig ventricular myocytes. *Journal of Physiology*, 552.(3):715–726, 2003.

[3] Lee A. Segel Evyatar Av-Ron, Hanna Parnas. A minimal biophyisical model for an excitable and oscillatory neuron. *Biological Cybernetics*, 1991.

[4] Lee A. Segel Evyatar Av-Ron, Hanna Parnas. A basical biophyisical model for bursting neurons. *Biological Cybernetics*, 1992.

[5] Robert A Gatenby and Robert J. Gilles. Why do cancer have high aerobic glycolysis? *Nature review*, 4:891–899, 2004.

[6] Marco Arieli Herrera-Valdez, Sandra Daniela Berger, Carsten Duch, and Sharon Crook. Diffferential contribution of k^+ channels to membrane excitability. *PLoS ONE (In review)*, 2010.

[7] Eugene M. Izhikevich. *Dynamical systems in neuroscience*. The MIT Press, 2007.

[8] L.P. Endresen A K. Hall A J.S. Huye A J. Myrheim. A theory for the membrane potential of living cells. *Eur Biophys J*, 1999.

[9] Burton David Rose and Theodore W. Post. *Clinical Physiology of Acid-Base and Electrolyte Disorders*. McGraw-Hill, 2001.

[10] O. Sotolongo-Costa, L. Morales Molina, D. Rodríguez Perez, J. C. Antoranz, and M. Chacón Reyes. Behavior of tumors under nonstationary therapy. *Physica D: Nonlinear Phenomena*, 178:242–253, April 2003.

[11] Steven H. Strogatz. *Nonlinear Dynamics and Chaos*. Perseus Books Publishing, L.L.C, Reading, Massachusetts, 1994.

[12] John Wiley. *Proton Passage Across Cell Membrane*, volume 139. The Ciba Foundation, Chichester Foundation Symposia, 1988.

A Appendix

A.1 Derivation of the Nernst-Planck equation

$$\vec{\phi}_{total} = -ukT\nabla[S] - uzq[S]\nabla U \tag{74}$$

$$= -ukT\left(\exp\left(-\frac{zqU}{kT}\right)\exp\left(\frac{zqU}{kT}\right)\right)\nabla[S]$$

$$- ze[S]\left(\frac{ukT}{kT}\right)\left(\exp\left(-\frac{zqU}{kT}\right)\exp\left(\frac{zqU}{kT}\right)\right)\nabla U \tag{75}$$

$$= -ukT\exp\left(\frac{-zeU}{kT}\right)\left[\exp\left(\frac{zeU}{kT}\right)\nabla[S] + [S]\nabla\left(\exp\left(\frac{zqU}{kT}\right)\right)\right] \tag{76}$$

$$= -ukT\exp\left(-\frac{zqU}{kT}\right)\nabla\left[[S]\exp\left(\frac{zqU}{kT}\right)\right] \tag{77}$$

A.2 Phase plane plots

A.2.1 Software

The programs which generated our phase plane plots were written using freely available software. The programming language used was Python (www.python.org), with the following packages being employed: SciPy (www.scipy.org), PyLab (www.scipy.org/PyLab), and SymPy (docs.sympy.org).

A.2.2 Nullclines

Our system of equations for no input current is:

$$\frac{dv}{dt} = F(v,w) = -\frac{a_{\mathrm{Na}}}{c_m} m_\infty^3(v) \sinh\left(\frac{q}{2kT}(v - v_{\mathrm{Na}})\right) - \frac{a_K}{c_m} w^4 \sinh\left(\frac{q}{2kT}(v - v_{\mathrm{K}})\right) \tag{78}$$

$$\frac{dw}{dt} = G(v,w) = \frac{w_\infty(v) - w}{\tau_w(v)} \tag{79}$$

where,

$$m_\infty(v) = \left[1 + \exp\left(\frac{z_m q}{kT}(v_m - v)\right)\right]^{-1} \tag{80}$$

$$w_\infty(v) = \left[1 + \exp\left(\frac{z_w q}{kT}(v_w - v)\right)\right]^{-1} \tag{81}$$

$$\tau_w(v) = \left[2 r_w \cosh\left(\frac{z_w q}{2kT}(v_w - v)\right)\right]^{-1}. \tag{82}$$

If we set the RHS of both (79) and (80) to zero, we obtain equations $F(w,v) = 0$ and $G(w,v) = 0$, respectively, for two curves in the w,v-phase plane - the v and w nullclines of our system (79), (80). To plot these curves, we set v in $F(w,v) = 0$ and $G(w,v) = 0$ to a value v_0 in the physiological range between the negative-valued Nernst potential v_{K} of potassium and the Nernst potential v_{Na} of sodium (≈ -75 and ≈ 65, respectively, for the temperatures of our simulation). This yields two equations $F(w,v_0) = 0$ and $G(w,v_0) = 0$ in w. These are solved for the w_0 corresponding to v_0 by using the function `scipy.optimize.fsolve()` in the SciPy package. This process is continued until all points (w,v) of each nullcline, where v is one of a discrete set of values lying between v_{K} and v_{Na}, are determined. Note that w values are computed for given v values, and not vice-versa, because the v nullcline is single-valued as a function of v, but multi-valued as a function of w.

When the input current is switched on, a constant current term I_0 is added to the RHS of (79). This has the effect of altering the v nullcline

(the w nullcline remains unchanged). Hence, our plots display the v nullcline for no current as a dashed curve; the v nullcline while the input current is switched on is displayed as a solid curve. The v nullclines differ visibly in the lower left portion of the plots, where v is negative and w is less than 0.4.

A.2.3 Trajectories

The trajectories in the w, v-phase plane were obtained by solving our system of equations using the function `scipy.integrate.odeint()` in the SciPy package. (The parameter values used are those listed in Table 1 of Sec. 3.1.1.). The solution was found for the time interval 0 to 1000 ms. The input current was simulated by adding a function of time $I(t)$ to the RHS of (79), which was 0 at all times except from 500 to 600 ms, when it held the constant value 0.1 nA. The initial point was chosen close to the stable fixed point (intersection of the nullclines) existing while the current is switched off. We thereby modeled the behavior of the neuron's membrane potential, which remains close to a resting value until it is excited by a current of sufficient strength and duration.

A.3 Proof of mathematical equivalence in (38)-(39)

Lets depart from equation (39) and get to (38).

$$\lambda(T)\sqrt{[H]_0[Na]_0[H]_i[Na]_i}\sinh[(q/2kT)(-V_H + V_{Na})] \tag{83}$$

If we substitute the Nernst potential for H^+ and Na^+ into the previous expression we obtain the following

$$\lambda\sqrt{[H]_0[Na]_0[H]_i[Na]_i}\frac{-\frac{[H]_0[Na]_i}{[H]_i[Na]_0}+1}{2(\frac{[H]_0[Na]_i}{[H]_i[Na]_0})^{1/2}} \tag{84}$$

Consider $[H]_o = x$, $[H]_i = \phi$, $[Na]_{i,o} = \eta_{i,o}$. With these redefinitions we obtain

$$\frac{dx}{dt} = \lambda(T)\sqrt{x\eta_o\phi\eta_i}\frac{-\frac{x\eta_i}{\phi\eta_0}+1}{2(\frac{x\eta_i}{\phi\eta_0})^{1/2}}. \tag{85}$$

we finally obtain the desired expression with the new variable x, as follows

$$\lambda(T)(-x\eta_i + \phi\eta_0) \tag{86}$$

A.4 Proof of the graphical properties of V(x)

To analytically prove all these we made a few aesthetical changes to expression 55, as follows

$$V(x) = mx^3 + nx^2 - qx \tag{87}$$

where $m = \frac{PA_{x1}}{3} > 0$, $n = \frac{1}{2}(A_{y1}A_{x1} + PA_{y2} - PA_{x2})$ and $q = A_{y1}A_{x2} > 0$. Setting $V(x) = 0$ in (88), we obtain the following results for x:

$$x_o = 0 \tag{88}$$

$$x_{1,2} = -\frac{n}{2m} \pm \sqrt{(\frac{n}{2m})^2 + \frac{q}{m}} \tag{89}$$

where $\frac{q}{m} > 0$ implies that $\frac{n}{2m} < \sqrt{(\frac{n}{2m})^2 + \frac{q}{m}}$, and so we have one positive solution and one negative for each selection of sign in (90). We now find the extremes of the potential, so taking the derivative of (90) we find $\frac{dV(x)}{dx} = 0$, obtaining:

$$\frac{dV(x)}{dx} = 3mx^2 + 2nx - q = 0 \Rightarrow x_{1,2} = -\frac{2n}{6m} \pm \sqrt{(\frac{2n}{6m})^2 + \frac{q}{3m}}. \tag{90}$$

In order to find what type of extreme each of these previous solutions are, we plug it into $\frac{d^2V(x)}{dx^2}$ and find the sign for each entry.

$$\frac{d^2V(x)}{dx^2} = 6mx + 2n \tag{91}$$

$$\frac{d^2V(x_{1,2})}{dx^2} = 6m\left(-\frac{2n}{6m} \pm \sqrt{(\frac{2n}{6m})^2 + \frac{q}{3m}}\right) + 2n \tag{92}$$

$$= \pm 6m\sqrt{(\frac{2n}{6m})^2 + \frac{q}{3m}} \tag{93}$$

From this last result is clear that for the positive entry we will have a minimum and for the negative a maximum. With this is proved all the proposed above.